DEVELOPMENT AND VALIDATION OF THE THREE-DIMENSIONAL DYNAMIC CODE - KIKO3D

A. Keresztúri, Gy. Hegyi, M. Telbisz, I. Cs. Hegedus
KFKI Atomic Energy Research Institute
H-1525 Budapest 114, POB 49, Hungary
kere@sunserv.kfki.hu

ABSTRACT

A three-dimensional reactor dynamics program - KIKO3D - for coupled neutron kinetics and thermohydraulics calculation of VVER type pressurized water reactor cores has been developed and benchmarked. For solution of the time dependent neutronic equations, a nodal method has been elaborated which is general concerning the geometry, the symmetries of the nodes, and the concrete form of the neutronic equations to be solved inside the nodes (transport or diffusion equation). Only the linear anisotropy of neutron flux on the node boundaries is utilised. Generalized response matrices for the time dependent problem are introduced which can be derived also from the response matrix of the stationary problem. The obtained time dependent matrix equations show similar structure to the not discretized equations. Therefore, the Improved Quasi Static factorization of the time dependent matrix equations can be carried out in the usual way leading to the point kinetic and the shape function equations.

In the KIKO3D code, the above general nodal method was applied for the special case of rectangular and hexagonal homogenized nodes in which the diffusion equation is to be solved. In this special case, the traditional response matrices of the stationary problem and the generalized matrices necessary for the time dependent problem can be given by analytical formulas. The accuracy of the introduced approximations have been validated against rectangular and hexagonal benchmark problems.

1. INTRODUCTION

As the safety requirements of nuclear power plants have increased, three-dimensional calculations become necessary in transient and accident analyses. The VVER type pressurized water reactors differ from other light water reactors because of their hexagonal fuel assembly arrangement. Therefore special hexagonal three-dimensional dynamic codes were developed for the safety analyses of VVER reactors.

KIKO3D[1] is a three-dimensional reactor dynamics program for coupled neutron kinetics and thermohydraulics calculation of VVER type pressurized water reactor cores. The code has been developed in the KFKI Atomic Energy Research Institute. Main applications of KIKO3D are the calculations of asymmetric reactivity initiated accidents in the core, e.g. control rod ejection, start-up of inoperable loop, inadvertent control rod withdrawal. It was used already in the AGNES project[2] for some safety reassessment calculations of PAKS NPP.

The neutron-physical algorithm was verified by well known international mathematical benchmarks. The neutron-physical and thermohydraulical validation of the program was performed in the frame of the AER international VVER co-operation by the specification of new hexagonal VVER-440 type benchmark problems.

2. DESCRIPTION OF KIKO3D

KIKO3D[1] is a three-dimensional reactor dynamics program for coupled neutron kinetics and thermohydraulics. Main applications of KIKO3D are the calculation of asymmetric accidents in core, e.g. control rod ejection, start-up of inoperable loop, inadvertent control rod withdrawal. The above - so called - middle-fast transients play an important role in safety analyses. The modelling of the faster transients characterized by the pressure waves spreading at sonic velocity is out of the scope. The code is coupled with the stationary program system KARATE, by means of that the stationary state of the reactor before the transient can be calculated. The burnup distribution taken from KARATE is regarded to be constant during the middle fast transients.

KIKO3D is a nodal code, where the nodes are the hexagonal or rectangular fuel assemblies subdivided into axial layers. The typical numbers of assemblies and axial layers for a VVER-440 core are 349 and 10, respectively. The symmetries of full and 1/2 core can be used in the calculations. The thermohydraulics is calculated in separate axial hydraulic channels of the core, each of which relates to one fuel assembly. The conservation equations of mass, energy and momentum are solved for the liquid and vapour phases. In order to get an accurate representation of the temperature Doppler feed-back, a heat transfer calculation with several radial meshes is done for an average representative fuel rod in each node. The release of prompt and delayed nuclear heat in the fuel is modelled. In the present version of the code, the VVER-440 correlations are used in the thermohydraulical module.

The neutron kinetics model of KIKO3D can be summarized as follows:

- 2 energy groups.
- The nodes are the fuel assemblies subdivided by axial layers.
- The unknowns are the scalar flux integrals on the reactor node interfaces.

- Linear anisotropy of the angle dependent flux on the node boundaries is supposed. The scalar flux and net current integrals are continuos on the node interfaces.

- Analytical solutions of the diffusion equation inside the nodes. The two-group constants are paramterized according to the feed-back parameters, burnup, and the most important isotope concentrations.

- Generalized response matrices of the time dependent problem and time dependent nodal equations are used.

- IQS (Improved Quasi Static) factorization; shape function equations and point kinetic equations.

- The absorbers and the reflector are represented by precalculated albedo matrices depending on several parameters.

The KIKO3D code is coupled to the ATHLET system thermohydraulic code[3]. There are two possibilities of parallel running of the KIKO3D code to the ATHLET thermohydraulic program:

- Coupling of 3D neutronics models to the system code that models completely the thermohydraulics in the primary circuit including the core region. In this case ATHLET obtains the heat source from the decay heat model of KIKO3D. The fuel and moderator temperatures, moderator densities, boron concentrations necessary for the feedback in KIKO3D originate from the ATHLET program. The drawback of this method is that the assumed discretization of the system thermohydraulic code is too coarse to take into account the node wise feed-back effects.

- Parallel running of the two programs. In this case, the KIKO3D code obtains the inlet flow rate, enthalpy, boron concentration distribution and the outlet pressure from the ATHLET code. The latter program also performs calculations in the core. The time dependent heat source distributions are calculated by the KIKO3D.

2. NODAL NEUTRON KINETIC EQUATIONS

The core is subdivided into nodes. Six delayed neutron groups are considered. The time dependent neutron balance in each node is written into the following form:

$$\hat{\mathbf{T}}(\mathbf{r},t)\Psi(\mathbf{r},t) = \left(\frac{1}{\mathbf{v}}\frac{\partial}{\partial t} - c\,b\,\hat{\mathbf{F}}\right)\Psi(\mathbf{r},t) + c\sum_{j=1}^{6} l_j C_j(\mathbf{r},t)\ , \qquad (1a)$$

$$\frac{dC_j(\mathbf{r},t)}{dt} = -l_j C_j(\mathbf{r},t) + b_j \hat{\mathbf{F}}\Psi(\mathbf{r},t)\ , \qquad (1b)$$

where

$\hat{\mathbf{T}}$ comprises the terms of the static neutronic equation (for example the two-group diffusion equation),

$\hat{\mathbf{F}}$ is the fission operator,

$\Psi(\mathbf{r},t)$ is the two-group scalar flux,

β_j and β are the delayed neutron fractions,

$C_j(\mathbf{r},t)$ are the precursor densities,

χ is the fission spectrum.

The solution of Eq.(1) is searched in each node as the linear combination of three terms: Φ_0, Φ_a, Φ_f. The first term (Φ_0) corresponds to zero source in Eq. (1a) and unity face integrated fluxes on the nodes boundary. The second and third term approximately corresponds to the respective source in Eq. (1a) and zero boundary fluxes. The corresponding solutions are Φ_a and Φ_f with sources according to the following definitions:

$$\hat{\mathbf{T}}(\mathbf{r},t)\Phi_0(\mathbf{r},t)=0\,, \qquad \Phi^{gg'}_{0kk'}=\delta_{kk'}\delta_{gg'}\,,$$

$$\hat{\mathbf{T}}(\mathbf{r},t)\Phi_a(\mathbf{r},t)=\frac{1}{\mathbf{v}}\Phi_0(\mathbf{r},t), \qquad \Phi^{gg'}_{akk'}=0\,,$$

$$\hat{\mathbf{T}}(\mathbf{r},t)\Phi_f(\mathbf{r},t)=\chi\hat{\mathbf{F}}\Phi_0(\mathbf{r},t), \qquad \Phi^{gg'}_{fkk'}=0\,,$$

where $\Phi^{gg'}_{xkk'}$ (x = "0", "a", "f") are the scalar flux integrals on the node boundaries in the group "g" and on the boundary "k". The number of the solutions of each type is equal to the number of the node boundaries multiplied by the number of the energy groups. The different solutions are denoted by the indices " k' " and " g' ". (These indices for Φ_0, Φ_a and Φ_f are omitted.)

The following approximations are applied in the right side of Eq. (1a), which is the driving term of the deviation from the stationary solution:

$$C_j(\mathbf{r},t)\approx\sum_{k',g'}\tilde{O}^{g'}_{jk'}\hat{\mathbf{F}}\Phi_0(\mathbf{r},t,k',g')\,,$$

$$\Psi(\mathbf{r},t)\approx\sum_{k',g'}\tilde{F}^{g'}_{k'}\Phi_0(\mathbf{r},t,k',g')\,,$$

$$\frac{d}{dt}\Psi(\mathbf{r},t)\approx\sum_{k',g'}\frac{d\tilde{F}^{g'}_{k'}}{dt}\Phi_0(\mathbf{r},t,k',g')\,,$$

where $\tilde{F}_{k'}^{g'}$ are the scalar flux integrals on the node boundaries, and $\tilde{O}_{jk'}^{g'}$ are amplitudes of the precursor distributions.
Using the approximations described above the solution of Eq. (1a) can be expressed in the form:

$$\Psi(\mathbf{r},t) = \sum_{k'g'}\left[\tilde{F}_{k'}^{g'}\left(\Phi_{\mathbf{0}}(\mathbf{r},t,k',g') - b \quad \Phi_{\mathrm{f}}(\mathbf{r},t,k',g')\right) + \frac{d\tilde{F}_{k'}^{g'}}{dt}\Phi_{a}(\mathbf{r},t,k',g')\right] +$$
$$+ \sum_{j=1}^{6} l_{\mathrm{j}} \sum_{k'g'} \tilde{O}_{\mathrm{j}k'}^{g'}\Phi_{\mathrm{f}}(\mathbf{r},t,k',g')$$

We introduce the generalized response matrices associated with each function giving the amount of face integrated currents at the node boundaries either due to a unit flux on the node boundary or due to a volumetric source:

$$\tilde{G}_{xkk'}^{gg'} = -\int_{\P k} D^{g}\, grad\, \Phi_{x}(\mathbf{r},t,k',g')d^{2}\mathbf{r} \ , \qquad (\mathrm{x} = \text{"0"}, \text{" } a \text{ ", "f"}) \ . \tag{2}$$

With the help of the above defined response matrices, the face averaged net currents are expressed as a linear expression of the volumetric sources and face averaged fluxes:

$$J_{k}^{g} = \sum_{k'g'}\left[\tilde{F}_{k'}^{g'}\left(\tilde{G}_{0kk'}^{gg'} - b\tilde{G}_{fkk'}^{gg'}\right) + \frac{d\tilde{F}_{k'}^{g'}}{dt}G_{akk'}^{gg'}\right] + \sum_{j=1}^{6} l_{j} \sum_{k'g'} \tilde{O}_{\mathrm{j}k'}^{g'}\tilde{G}_{fkk'}^{gg'} \ .$$

Using the continuity of currents on the common boundaries of the adjacent nodes, the time dependent nodal equation for the whole reactor can be derived, where the unknowns are the time dependent amplitudes $O_{jk'}^{g'}$ and the face integrated fluxes $F_{k'}^{g'}$:

$$\sum_{k'g'}\left[\left(G_{okk'}^{gg'} - b\,G_{fkk'}^{gg'}\right)F_{k'}^{g'} + \sum_{\mathrm{j}=1}^{6} l_{\mathrm{j}}\, G_{fkk'}^{gg'} O_{\mathrm{j}k'}^{g'} + G_{akk'}^{gg'}\frac{d}{dt}F_{k'}^{g'}\right] = 0 \ , \tag{3a}$$

$$\frac{d}{dt}O_{\mathrm{j}k}^{g} = -\,l_{\mathrm{j}}O_{\mathrm{j}k}^{g} + b_{\mathrm{j}}F_{k}^{g} \ . \tag{3b}$$

In these equations the maximum value of indices k and k' is equal to the number of boundaries between the nodes and on the edge of the reactor. The quantities $\mathbf{G_x}, \mathbf{O}, \mathbf{F}$ related to the entire reactor are defined by using the geometrical connections between the nodes. The definitions of $\mathbf{O}$ and $\mathbf{F}$ are the same as that of $\tilde{\mathbf{O}}$ and $\tilde{\mathbf{F}}$ related to the individual nodes, but they are numbered

according to the entire reactor. Eqs. (3) and $\mathbf{G_x}$ are obtained from $\tilde{\mathbf{G}}_\mathbf{x}$ taking into account the continuity of the net current on the node boundaries, which can be expressed from both sides of the adjacent nodes.

The factorization of the improved quasi static (IQS) method is introduced as

$$\mathbf{F}(t) = A(t)\mathbf{f}(t),$$

where $A(t)$ is the amplitude function, and $\mathbf{f}(t)$ is the shape function changing slowly with the time according to its normalisation:

$$\frac{d}{dt}(\mathbf{W},\mathbf{G}_a\mathbf{f}) = \mathbf{0}.$$

Substituting the above expression of $\mathbf{F}(t)$ into Eq. (3) the following compact form is obtained for the shape factor equation:

$$\left(\mathbf{G_0} - b\mathbf{G_f} - \frac{\frac{dA}{dt}}{A}\mathbf{G}_a \right)\mathbf{f} - \mathbf{G}_a \frac{d\mathbf{f}}{dt} + \frac{1}{A}\sum_{\mathbf{j}=1}^{6} l_\mathbf{j}\mathbf{G_f}\mathbf{O_j} = \mathbf{0}. \qquad (4)$$

Using the above equation and Eq. (3b) for the time independent case, the following equation is obtained for the shape function at the beginning of the transient (t=0):

$$\mathbf{G_0}(t=0)\mathbf{f} = \mathbf{0},$$

and for its adjoint:

$$\mathbf{G_0^*}(t=0)\mathbf{W} = \mathbf{0}.$$

($\mathbf{G_0^*}$ is the transpose of $\mathbf{G_0}$.)

After the substitution of the factorized form, multiplying Eq. (3) by the adjoint weight function $\mathbf{W}$, evaluating the sum over the node boundaries and over the energy groups, the equations for the amplitude function and for the core averaged precursor densities - the point kinetic equations - are obtained:

$$\frac{dA}{dt}(\mathbf{W},\mathbf{G}_a\mathbf{f}) = A((\mathbf{W},\mathbf{G_0}\mathbf{f}) - b(\mathbf{W},\mathbf{G_f}\mathbf{f})) + \sum_{\mathbf{j}=1}^{6} l_\mathbf{j}(\mathbf{W},\mathbf{G_f}\mathbf{O_j}) + A(\mathbf{W},\frac{d\mathbf{G}_a}{dt}\mathbf{f}), \qquad (5)$$

where $A(t=0) = 1,$

$$\frac{d}{dt}(\mathbf{W},\mathbf{G_f}\mathrm{O_j}) = -\,l_j(\mathbf{W},\mathbf{G_f}\mathrm{O_j}) + b_j(\mathbf{W},\mathbf{G_f}\mathbf{f})A + (\mathbf{W},\frac{d\mathbf{G_f}}{dt}\mathrm{O_j}). \qquad (6)$$

Equations (3b), (4), (5) and (6) form a close set to be solved.

Another possible derivation of the response matrices defined in Eq. (2) can be obtained by introducing $\tilde{\mathbf{T}} = \hat{\mathbf{T}} + \frac{a}{\mathbf{v}} + rc\hat{\mathbf{F}}$ instead of the original $\hat{\mathbf{T}}$ in (1). Following the above procedure for $\tilde{\mathbf{G}}_\mathbf{0}$, the basic response matrix used in the stationary problem will be the function of r and a:

$$\hat{\mathbf{G}}_\mathbf{0} = \hat{\mathbf{G}}_\mathbf{0}(a,r).$$

From the definition of $\mathrm{F}_\mathbf{0}$, F_a and F_f it can be proved that the generalized response matrices can be derived from the steady state response matrix in the following way:

$$\tilde{\mathbf{G}}_a = \frac{\partial}{\partial a}\hat{\mathbf{G}}_\mathbf{0} \qquad\qquad \tilde{\mathbf{G}}_\mathbf{f} = \frac{\partial}{\partial r}\hat{\mathbf{G}}_\mathbf{0}\ .$$

Up to this point, the theory is entirely general. The geometry is arbitrary, and the nodes could be heterogeneous.

In the KIKO3D program, the above described method is used for the special case of the homogenized hexagonal and rectangular nodes. For the homogenized nodes, analytic expressions of exponential and trigonometric functions can be used in the solutions, and the response matrices can be calculated in an analytic way[1].

3. NUMERICAL METHODS

Two types of time steps are applied in KIKO3D according to the IQS (Improved Quasi Static) method. In each micro time step the point kinetic equations (5) and (6) are integrated, and the fuel heat transfer equations are solved for each node. In the macro time steps the response matrices and its derivatives are calculated, the precursor and shape function equations (Eqs. (3b) and (4)) are solved, and the hydraulic module is called. Practically, the computing time of the models called in each micro time step is negligible as compared to that of the macro time steps.

The point kinetic equations give a stiff ordinary differential equation, which is solved by the GRK4A stiff solver of Kaps and Rentrop. The shape function equations give the task to solve a large sparse linear system. It is dealt with standard large sparse techniques, where Gauss-Seidel preconditioning and a GMRES-type solver are applied. A block arrangement of the system makes it possible to iterate only for half size matrices.

4. VALIDATION OF THE NEUTRONIC MODEL

The validation of the neutronic model was performed step by step. The approximations are very similar in the different geometries, hence the verification could be started by well known benchmarks in simple geometries. At first homogenous bare reactor problems were solved which had analytical exponential solutions in slab geometry. Then international "mathematical" kinetic benchmark problems were calculated without feedback effects in square geometry.

Concerning the hexagonal geometry, first a 3D static hexagonal benchmark problem was solved. At the beginning, no internationally recognized hexagonal kinetic benchmarks were available for the validation of the code. The elaboration of such benchmarks and the exchange of information on the validation process was organized in the frame of Atomic Energy Research (AER) co-operation (Bulgaria, Czech Republic, Finland, Germany, Hungary, Poland, Russia and Slovakia). A series of hexagonal VVER benchmarks were built up during 1992-1997, first a relatively simple one and then gradually more complicate problems.

4.1 THE LMW (LANGENBUCH, MAURER, WERNER) KINETIC TEST PROBLEM[4]

This problem simulates a super delayed-critical operational transient in a LWR for a very small reactivity insertion rate in square geometry. Control rods are divided into two groups, the transient is initiated by the withdrawal of the first group, then negative reactivity is given by inserting the second group. The velocity of the absorbers is 3 cm/s, the size of the core is 220*220*200 cm, the transient is followed until 60 s. Maximum of reactivity is about 0.2 $.

The reference solution was calculated by the CUBBOX code with dt=0.125 s time steps[5]. The IQS method in KIKO3D code made it possible to use larger time steps. Time steps of dt=1.111 s and node sizes of 20*20*10 cm were used, but other time steps and point kinetic approximation were analyzed, too. The time dependence of the average power as well as the power densities at some places of the reactor were compared[6].

Fig. 1 shows the time dependence of the average power for KIKO3D and for CUBBOX. It contains the result of the point kinetic approximation too marked as KIKO3D-PK. KIKO3D results belonging to the relatively large time step of dt=1.111 s are in good agreement with the reference solution, while the point kinetic method strongly underestimates the power. The power densities at different places of the core show similar agreement.

The deviations of the average power from the reference solution at the time of maximum are as follows:

KIKO3D dt=1.111 s - dP/P= 2.7 %

KIKO3D dt=6.666 s - dP/P= 4.2 %
PK point kinetics - dP/P= 9.2 %

The above results verify the nodal method for square geometry and IQS method for small reactivity changes.

4.2 THE THREE-DIMENSIONAL HWR (Judd an Rouben) kinetic problem[5]

This problem simulates a LOCA in a CANDU-type PHWR in square geometry, followed by an asymmetric insertion of reactivity devices. The accident is simulated by given linear decrease in the thermal absorption, the motion of the absorber rods in the horizontal (-Y) direction is beginning at 0.6 s. The time of the transient is 2.5 s. Different node sizes were used in KIKO3D, 60 cm inside the core and 30 cm beside the reflector. Maximum of reactivity is near to the 1 $. The size of the reactor core is extremely large 780*780*800 cm, the perturbations have a strong asymmetry.

The reference solution[5] was calculated by the CERKIN code. Average power of reactor and thermal flux shapes were compared during the transient[6]. Fig. 2 shows the time dependence of the average power for KIKO3D and for CERKIN. The thermal flux shapes belonging to different codes are compared in Fig. 3. at time points t=0.0 s and t=0.9 s. The flux shape is given in direction X, at Y=360 cm and Z=270 cm.

The difference in the static multiplication factor is 0.07 %, the static thermal fluxes agree well. The very large size of the absorber rods needs very little time step dt=0.0125 s and needs the application of the predictor-corrector method in the flux shape calculations. The average power during the transient does not show any difference before the power maximum, but after this time the KIKO3D results are below the CERKIN results, the differences are about 2-3 % .

4.3 THE THREE-DIMENSIONAL VVER-TYPE STATIC PROBLEM[7] (SEIDEL, GRUNDMANN)

In this benchmark the 30° sector of a hexagonal VVER-440 reactor core is investigated, containing fuel assemblies of three different enrichments, absorber assemblies with followers, radial and axial reflectors and extrapolation lengths.

The reference solution was calculated by the fine-mesh OSCAR code. KIKO3D calculations were performed in 180° sector of the core with albedo boundary conditions. Table I. below contains the effective multiplication factors calculated by different codes:

Table 1. Calculated Effective Multiplication Factors

CODE	Rad. mesh size	Ax. mesh size	keff
OSCAR033	2.829 cm	5.0 cm	1.0124
FEM3	8.487 cm	25.0 cm	1.0132
HEXNOD23 H3	14.70 cm	6.25 cm	1.0116
KIKO3D	14.70 cm	25.0 cm	1.0120

The deviations of KIKO3D radial power distributions (k_q) from the reference solution are shown in Fig. 4. The k_q differences are less than 1.6 % , the agreement is good even beside the reflector.

These results verify the accuracy of the hexagonal steady state nodal method.

4.4 VALIDATION OF KIKO3D VVER-440 MODEL BY THE "AER" BENCHMARK PROBLEMS

With respect to the geometry, these problems are based on the static hexagonal VVER case given in 4.3. The first three benchmarks are asymmetric rod ejections from low power level, containing more and more complicate feedback calculations. The fourth problem is directed mostly for the investigation of the interaction between neutron kinetics and core thermohydraulics, the initial event is boron dilution and cooling disturbance of the coolant.

4.4.1 THE AER-1 BENCHMARK[8]

The aim is the validation of 3D neutron kinetics calculations for VVER-440 without any feedback. The transient is an asymmetric control rod ejection. It has two variants for the handling of control assemblies by two-group constants (A) or by albedo matrices (B). In case (A) cross sections of the rod are given in the benchmark, in case (B) the static reactivity of the control rod is given. The worth of the ejected rod is just below the prompt critical value. The equivalent cross sections and albedos for benchmark 1B were calculated by KIKO3D in stationary state. The reactivity worth of the ejected rod was 0.00482. The initial power is near to zero (HZP EOC), power rise is not too large, therefore the transient can be treated without feedback.

With respect to the geometry and the two-group constants, the problem is based on the 3D static hexagonal benchmark described by Seidel and Grundmann[7]. The initial axial position of control rods and the values of the production cross sections are slightly changed in order to reach the desired reactivity change.

The horizontal cross section of the core with material distribution is shown in Fig. 5. The lattice pitch is 14.7 cm. Type numbers 21,23,25,26 represent positions where either absorber assemblies or their followers can be placed. Albedo boundary condition is applied on the outer edge of the reflector nodes. Height of core is 250 cm, initial position of control rod groups 21 and 26 is 50 cm from the bottom of the core. The absorber groups No. 23 and 25 are out of core at the beginning of the transient. Control rod No. 26 is ejected from 0.0 s to 0.08 s, constant velocity is assumed. The drop of safety rods 23 and 25 is started at 1.0 s, and finished at 11.0 s. The drop of control rod group 21 is started also at 1.0 s. The transient is followed until 6.0 s.

In variant "A", three different calculations were compared[9, 10]: two DYN3D[11] calculations performed at FZR Rossendorf and KAB Berlin, and KIKO3D calculations. Due to the factorization method in KIKO3D, the form factors of the flux distribution could be calculated relatively rarely, when the position of the absorber rods corresponded to the node boundaries, so homogenisation of rod tips was not needed. In DYN3D model the homogenisation of the nodes containing both absorber and fuel was necessary because of the smaller time steps. A more advanced homogenisation method was applied in the Rossendorf calculation than that of KAB. Consequently, in the KAB calculation the fuel assemblies had to be subdivided into 12 nodes (+ 2 axial reflector nodes) in contrast to the KIKO3D and Rossendorf version of DYN3D, where 10 axial nodes per fuel assembly was used.

The results of KIKO3D and DYN3D were compared with the adiabatic results (see Figs. 6,7). In the adiabatic solution the reactivity was determined solving the eigenvalue problem for k_{eff} at the given configuration of the core, and the obtained time dependent reactivity was used in the point kinetic model. The large deviation of average core power for the adiabatic result (Fig. 6) shows that the solution is very sensitive to the small changes in the flux distribution and the reactivity (Fig. 7).

The agreement between KIKO3D and DYN3D power results is good, taking into account the large sensitivity (Figs. 6-8). The effect of homogenisation can be seen in the waving character of the DYN3D curves.

The node-wise power density distributions were compared in stationary case and in kinetic calculations at five different time points. The radial and axial power density distributions were quite the same for every solutions of 1A and 1B. The greatest differences between the solutions were observed at the end of the transient (t=6 s). Then the maximum deviation was 4 % between KIKO3D and DYN3D at the fuel assembly next to the ejected rod, as it can be seen at position 203 in Fig. 8.

Variant "B" was solved by 4 different codes[10]: DYN3D/FZR, KIKO3D, HEXTRAN[12], BIPR-8[13]. KIKO3D and DYN3D/FZR calculations agree well according to the similar handling of control rod. The HEXTRAN and BIPR8 results are somewhat different from KIKO3D and DYN3D results due to the deviations in the handling of control rod. It seems, that very small differences in the stationary results can cause significant deviations in dynamic behaviour of rod ejection transients.

4.4.2 THE AER-2 BENCHMARK[14]

The aim is the validation of 3D neutron kinetics calculations for VVER-440 with a simple adiabatic fuel temperature feedback mechanism.

The AER-1 benchmark is modified to obtain a stronger reactivity effect, the worth of the ejected rod is changed to 2$. The Doppler effect being the main feedback for this type of transients is the only feedback and it is taken into account by an adiabatic model of the fuel temperature. No heat is transferred from fuel to coolant. The rod is ejected during the first 0.16 s, the transient is followed until 2 s without scram.

The solution of KIKO3D and the detailed comparison with other solutions of DYN3D, HEXTRAN, BIPR8 can be found in references 15 and 16. The agreement of the results is quite satisfactory, however there exists some discrepancies due to the different handling of the absorbers. KIKO3D is able to use both cross sections and albedos. It was used to calculate equivalent albedos giving nearly the same eigenvalue and rod reactivity at the KIKO3D initial state. KIKO3D and DYN3D give approximately the same reactivity, while HEXTRAN and BIPR8 give a higher value (about 3%). The higher reactivity value results in a higher and earlier power peak, which can be seen in Fig. 9. The power peaks of KIKO3D and DYN3D have nearly the same maximum value. Fig. 10 shows the maximum fuel temperatures, the difference between the two pairs of codes is about 150°C, it is caused by the difference in the global power peaks.

4.4.3 THE AER-3 BENCHMARK[17]

The aim is the validation of coupled 3D neutron kinetic and thermohydraulic core calculations for VVER-440 including thermohydraulic feedback effects and whole core hydraulics. Realistic fuel temperature and moderator temperature feedback parameters are given. Except some simplifications the problem represents a realistic transient in a VVER-440 reactor.

It is a further extension of the previous rod ejection benchmark problems. The reactivity worth of the ejected rod is fixed at 1.9668 $. (This value is obtained in each code by the adjustment of cross sections or albedos for the control rod.) The ejection time is 0.16 s, the calculation is continued until time t=10 s. Reactor trip is not included in the calculation, hence a new steady state is achieved after the transient. The thermohydraulic feedback effects and the whole hydraulic of the core is included in the benchmark. The transient occurs in HZP EOC initial conditions with characteristic strong negative coolant temperature feedback and in flow conditions with only half of reactor coolant pumps on. The fuel heat transfer model includes prescribed temperature dependent fuel, gas gap and cladding properties. The core inlet conditions remain constant during the transient. The inlet temperature is 260°C. The fuel temperature and moderator temperature feedback coefficients and the recommended hydraulic correlations are given. A hot channel study with K_x =1.25 excess power peaking factor and with DNB (departure from nucleate boiling) calculation is also included in the benchmark.

The benchmark was calculated in 5 countries with 4 different codes[18,19]: KIKO3D, DYN3D/FZR, DYN3D/REZ, BIPR8, HEXTRAN. Hot channel calculation is not included in KIKO3D, this

calculation was performed by the TRABCO one-dimensional hot channel code based on the time dependent axial power density distributions from KIKO3D.

Figs. 11,12 show some samples from the results detailed in references 18 and 19. Fig. 11 shows the maximum node-wise fuel centerline temperatures calculated by KIKO3D, HEXTRAN and DYN3D/REZ and the maximum fuel centerline temperatures from the hot channel calculations with K_x=1.25 power peaking factor. Fig. 12 shows the axial power density distributions at different times in the hottest assembly calculated by KIKO3D and HEXTRAN.

The agreement between the relative power distributions belonging to different codes were rather good at the initial state and the later deviations during the transient were reasonable considering the differences in thermohydraulic models. The maximum fuel centerline temperatures of average rods agreed well, as it can be seen in lower part of Fig. 11.

Comparison of sensitive local quantities revealed some further differences between the codes. The power distributions were close to each other in the early phase of the transient, when moderator feedback was not yet significant and in the later phase at the new steady state. However, local deviations appeared in power distributions at the time of maximum boiling (t=1.5 s) in the neighbourhood of the ejected rod. Maximum of void fraction was underestimated in KIKO3D, it could be seen also in the axial distributions of coolant density and relative power of the hottest fuel assembly (See Fig. 12). The possible reasons of the deviation were analyzed.

As the applied thermohydraulic approximations in KIKO3D were not entirely in coincidence with the benchmark definition, the effects of different thermohydraulic options were investigated. The fuel heat transfer model corresponded exactly to the benchmark definition, but the hydraulic model was different. In the benchmark definition a non-equilibrium bulk void production and condensation model was defined supposing separate mass conservation equations for the two phases. KIKO3D has a COBRA3 type hydraulic model, the conservation equations are solved only for the mixture of liquid and vapour. The effects of several different boiling correlation were investigated. The other difference in the hydraulic model was the application of the specified pressure loss model. This model would have been a too serious modification in the code, therefore our realistic method developed for VVER-440 reactors was applied. The TRABCO hot channel code - by using unit hot channel factor - was suitable for methodical tests of the COBRA3 model, because its hydraulic model was in accordance with the benchmark specification.

The conclusion of this methodical analysis was, that the investigated correlations had a great effect on the void content in the hottest assembly, nevertheless the influence on the average power and on the safety parameters were negligible. The pressure loss model had minor effect on the results.

An other reason of the smaller void content calculated by KIKO3D was the somewhat smaller power peak at the beginning of the transient. The power peak and the stabilized power at the end were slightly smaller than those from HEXTRAN and DYN3D, the largest deviation at the end of transient was smaller than 1% of nominal power. This effect can be seen in the lower part of Fig. 11, the KIKO3D fuel temperatures are slightly smaller than the other ones at the peak and at the end of the

transient. The reason was not clear because in case of AER-2 benchmark this effect was not observed. As a consequence, the heat transferred to the coolant was also smaller, this led to a smaller outlet void fraction in the hottest assembly.

The hot channel calculations with excess power peaking factor 1.25 were performed by TRABCO code based on the time-dependent axial power distribution of the hottest channel in KIKO3D. The safety related parameters, like minimum of DNB ratio, maximum fuel and clad temperatures were in good agreement with the results of other codes, in spite of the underestimation of the void fraction in the hot assembly. DNB occurred in the hot channel almost immediately after the power peak in each calculation, but after this different film boiling correlations were used in the codes. HEXTRAN and KIKO3D models did not predict any rewetting, while BIPR8 and DYN3D correlations predicted rewetting after a few seconds. This effect can be seen on the upper part of Fig. 11.

The agreement of the neutron kinetics results was very good. The reliability of the neutron kinetic parts of the different nodal codes using different methods has been confirmed by the first three AER benchmarks. However it was confirmed too that there is a good reason in accident analyses to use conservative overestimated reactivity worth for the ejected rod because of the sensitivity of the results.

Also the thermohydraulic results of KIKO3D, DYN3D and HEXTRAN were very similar, the agreement in the safety related parameters was satisfactory.

4.4.4 THE AER-4 BENCHMARK[20]

The aim is the validation of coupled 3D calculations for VVER-440 concentrating mostly on the interaction between neutron kinetic and thermohydraulic modelling of the core.

The transient is started by boron dilution and cooling disturbance of coolant in hot subcritical state with all control rods inserted. The time dependent factors and static overcriticality value of the cold diluted slug is given. The core inlet conditions are specified to eliminate the modelling of the primary circuit outside the core. The transient occurs in BOC conditions with high boron concentration and in flow condition with one reactor coolant pump on. The flow conditions are approximated with 60^0 symmetry in the core. The geometry is similar to the earlier benchmarks, but more realistic. The nuclear cross section data are not given, every participant can use their own data. The feedback coefficients and the total delayed fraction of the whole core are given for a reference state.

The prescribed reactivity data in the static reference state needed a tuning process, needed modifications in KIKO3D neutronic data[21]. Preliminary sensitivity investigations were made using a point model for neutronics and a boron transport model with constant coolant velocity. The results show that the only important neutronic parameter is the overcriticality, and the numerical diffusion in the boron transport model has a major influence on the results. According to this a new solution method was built in the code to reduce the effects of numerical diffusion on the boron dilution front[21]. The 3D results of the different boron models are compared in Figs. 13-14. The new improved model gives more sudden and faster change in the boron concentration. The difference between the two models is increasing upwards in the core. The traditional model gives a later and smaller power peak,

underestimates the power transferred to coolant. The difference is 3-4 % , it leads to 50 °C deviation in maximum fuel centerline temperature. The KIKO3D hot channel calculation belonging to the new boron model predicts a rapid decrease in the minimum of DNB ratio. It is not very far from the 1.3 limit but does not reach it (see Fig. 15).

Other participants are also investigating tuning effects and boron model hence at present only the first results are compared[22]. Reasonable good consistency is found between them, but there are still time shift and power peak discrepancies due to the different boron transport.

Getting over this benchmark we can say, that KIKO3D new boron transport model is more conservative hence more suitable for conservative safety calculations than the traditional method.

SUMMARY

A three-dimensional reactor dynamics program - KIKO3D - for coupled neutron kinetics and thermohydraulics calculation of VVER type pressurized water reactor cores has been developed and benchmarked. For solution of the time dependent neutronic equations, a general nodal method has been elaborated, which was applied for the special case of rectangular and hexagonal homogenized nodes in the KIKO3D program.

The accuracy of the introduced approximations have been validated against rectangular and hexagonal benchmark problems. The systematic solution and the comparative analysis of the presented benchmark series validated the adequacy of KIKO3D models for VVER reactors. Results of other independent codes verified the neutron kinetic solution. The agreement was good even with the application of relatively large time steps due to the factorization method.

The selected results demonstrated the capabilities of KIKO3D for safety analysis of VVER power plants. It is a best estimate code but methods for conservative distortion of the desired parameters has been developed in it. Solution of the realistic benchmark problems made an extensive analysis and improvement of some parts of the thermohydraulic model necessary. The final results were reliable and the accuracy of the safety related parameters was satisfactory.

REFERENCES

1. A. Kereszturi, L. Jakab: A Nodal Method for Solving the Time-Depending Diffusion Equation in the IQS Approximation. KFKI-1991-35/G report, 1991.

2. AGNES Project Executive Summary. Budapest, 1994.

3. G.Lerchl, H.Austregesilo: The ATHLET Code Documentation Package, GRS-P-1 / Vol. 1.: User's Manual, October, 1995.

4. Langenbuch, Maurer, Werner: Coarse Mesh Flux-Expansion Method for the Analysis of Space-Time effects in Large Light Water Reactor Cores. Nucl. Sci. and Eng., 63, 437-456, 1977.

5. Benchmark problem book. ANL-7416 (Supplement 3).

6. M. Telbisz, A. Keresztúri: The Benchmark Testing of KIKO-3D Three Dimensional Hexagonal Kinetic Code. Proc. of 2nd AER Symp., Paks Hungary, 1992.

7. U. Grundmann: HEXNOD-23 A Two- and Three-Dimensional Nodal Code for Neutron Flux Calculation of Thermal Reactors wit Hexagonal Geometry ZfK-557 report, 1985.

8. A. Kereszturi, M. Telbisz: A Three-Dimensional Hexagonal Kinetic Benchmark Problem, Proc. of 2nd AER Symp., Paks Hungary, 1992.

9. A. Keresztúri, M. Telbisz, I. Vidovszky, U. Grundmann, J. Krell: Results of a Three-Dimensional Hexagonal Kinetic Benchmark Problem, Proc. of ENS Meeting, Portoroz 1993.

10. M. Telbisz, A. Kereszturi: Results of a Three-Dimensional Hexagonal Kinetic Benchmark Problem, Proc. of the 3rd Symposium of AER, Piestany Slovakia, 1993.

11. Grundmann, U. Rohde: DYN3D/M2 a Code for Calculation of Reactivity Transients in Cores with Hexagonal Geometry, Report ZfK-690, Rossendorf, 1989.

12. Kyrki-Rajamaki R.: HEXTRAN VVER Reactor Dynamics Code for 3D Transients, Proc. of the 1st Symposium of AER 1991.

13. M. P. Lizorkin et al.: Time-depended Spatial Neutron Kinetic Algorithm for BIPR-8 and Its Verification, Proc. of 2nd AER Symp., Paks Hungary, 1992.

14. U. Grundmann, U. Rohde: Definition of the second kinetic benchmark of AER, Proc. of the 3rd Symposium of AER, Piestany Slovakia, 1993.

15. A. Kereszturi: Calculation of the second AER kinetic benchmark problem with KIKO3D, Proc. of the 4th Symposium of AER, Sozopol Bulgaria, 1994.

16. U. Grundmann: Results of second kinetic AER-benchmark, Proc. of the 4th Symposium of AER, Sozopol Bulgaria, 1994.

17. R. Kyrki Rajamaki, E. Kaloinen: Definition of the third three-dimensional hexagonal dynamic AER benchmark problem, Proc. of the 4th Symposium of AER, Piestany Slovakia, 1993.

18. A. Keresztúri, M. Telbisz, Gy. Gyenes: Calculation of the third three-dimensional hexagonal dynamic benchmark problem with KIKO3D, Proc. of the 6th Symp. of AER, Kirkkonummi Finland, 1996.

19. R. Kyrki-Rajamaki, U. Grundmann, A. Kereszturi: Results of three-dimensional hexagonal dynamic benchmark problems for VVER type reactors, Proc. of the PHYSOR 96, Mito, Ibaraki, Japan, 1996.

20. R. Kyrki-Rajamaki: Definition of the 4th dynamic benchmark, Proceedings of the 6th Symposium of AER, Kirkkonummi, 1996.

21. A. Keresztúri, M. Telbisz, Gy. Gyenes: Calculation of the fourth AER kinetic benchmark problem with KIKO3D, Proc. of the 7th Symp. of AER, Hornitz Germany, 1997.

22. R. Kyrki-Rajamaki: Comparison of the first results of the fourth hexagonal dynamic AER benchmark problem, boron dilution in core, Proc. of the 7th Symp. of AER, Hornitz Germany, 1997
M. Telbisz, A. Kereszturi: Results of a Three-Dimensional Hexagonal Kinetic Benchmark Problem, Proc. of the 3rd Symposium of AER, Piestany Slovakia, 1993.

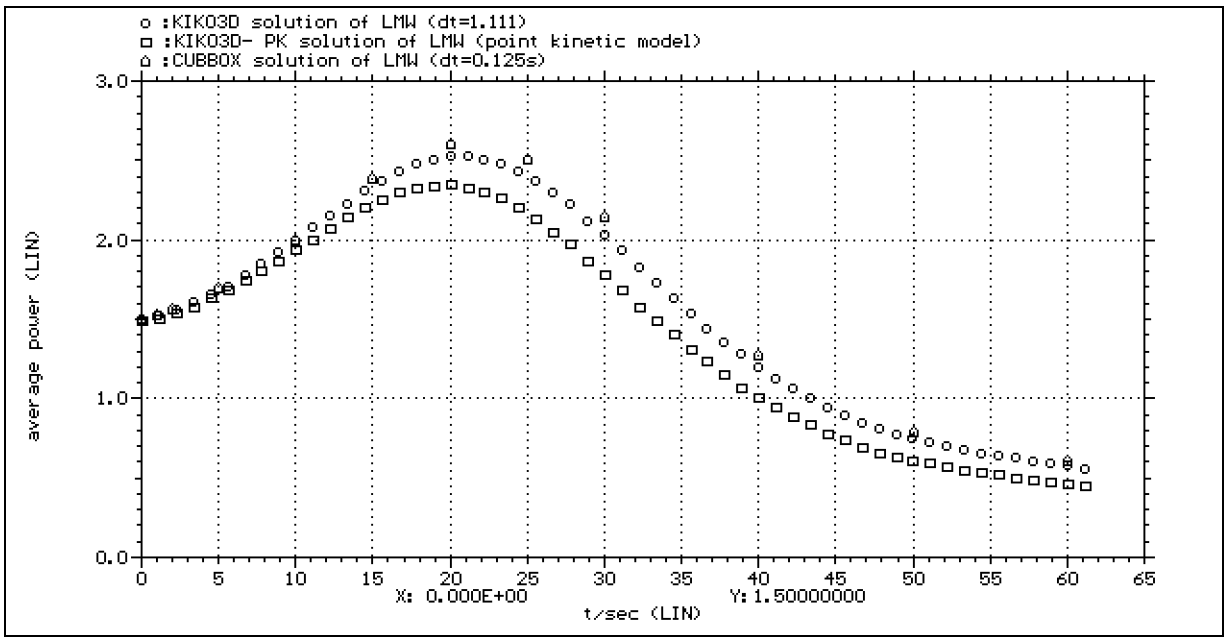

Fig. 1. Comparison of Average Power in the LMW Test Problem

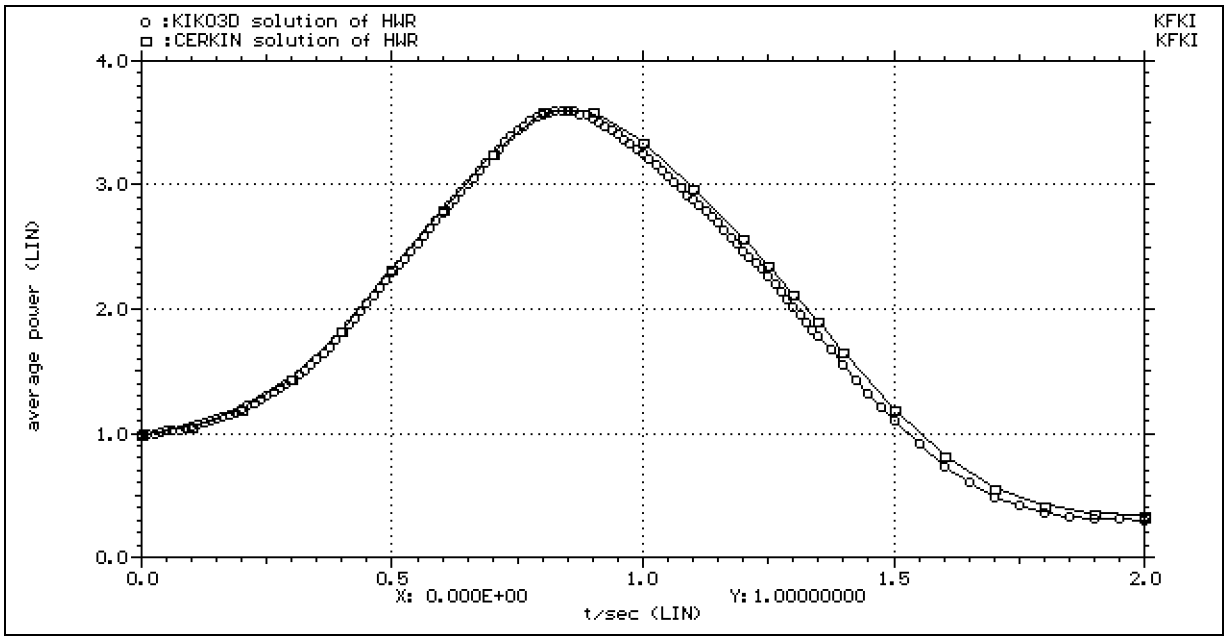

Fig. 2. Comparison of Average Power in the HWR Test Problem

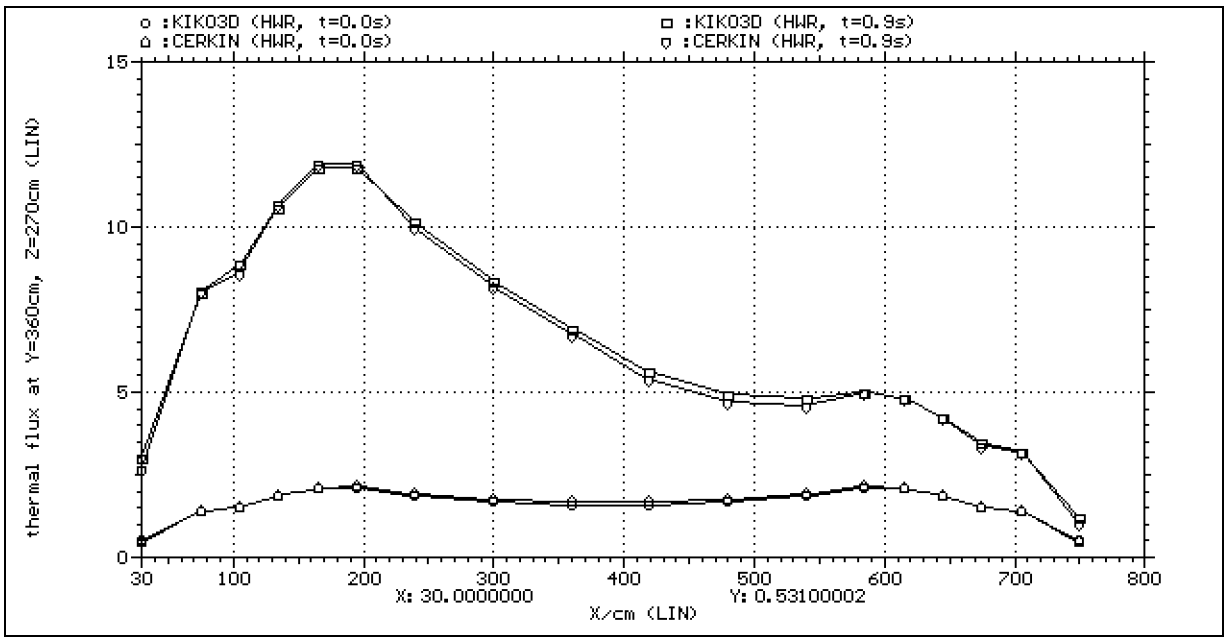

Fig. 3. Comparison of Thermal Flux Shapes in X Direction Belonging to t=0.0 s and t=0.9 s in the HWR Test Problem

0.0

-0.9 -0.7 0.0

0.2 -0.3 -0.5 -0.7 0.0

1.1 0.3 -0.1 -0.7 -0.4 0.0 0.0

1.4 0.8 0.6 0.5 0.0 -0.3 -0.6 0.0 0.0

1.5 1.1 1.3 1.1 0.6 -0.2 -0.8 -0.5 -0.6 0.0 0.0

1.6 1.2 1.5 1.5 0.9 0.5 -0.1 0.0 -0.2 -0.9 0.0 0.0 0.0

Fig. 4. Relative k_q Differences (%) in a 30^o Symmetry Sector of the Static VVER Test Problem

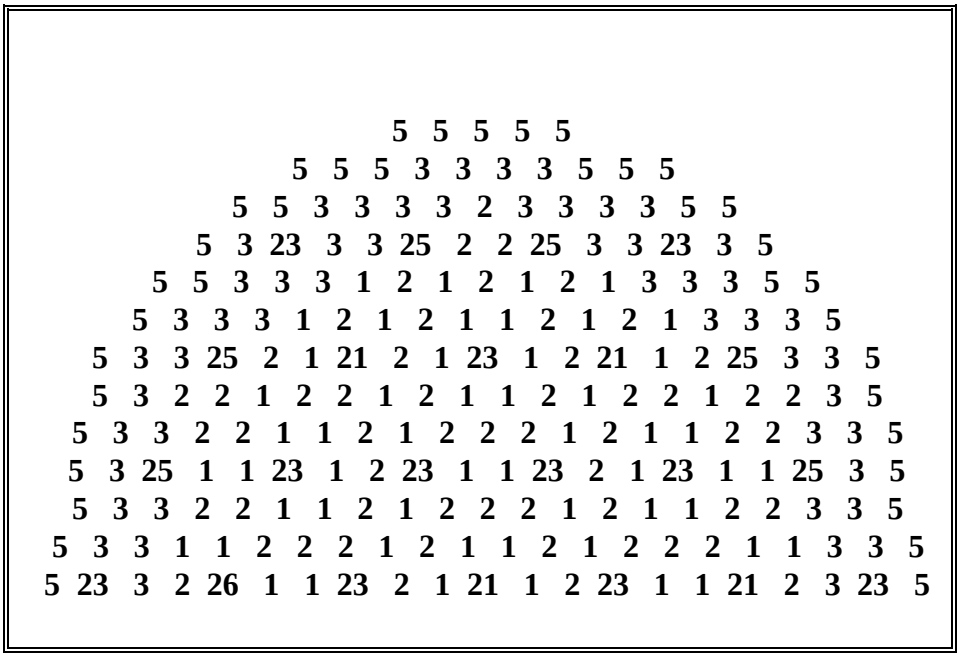

Fig. 5. Horizontal Cross Section of VVER-440 Half Core With Material Numbers Used in the AER Benchmarks. Reflector Nodes Marked by No. 5. Ejected Rod Marked by No. 26.

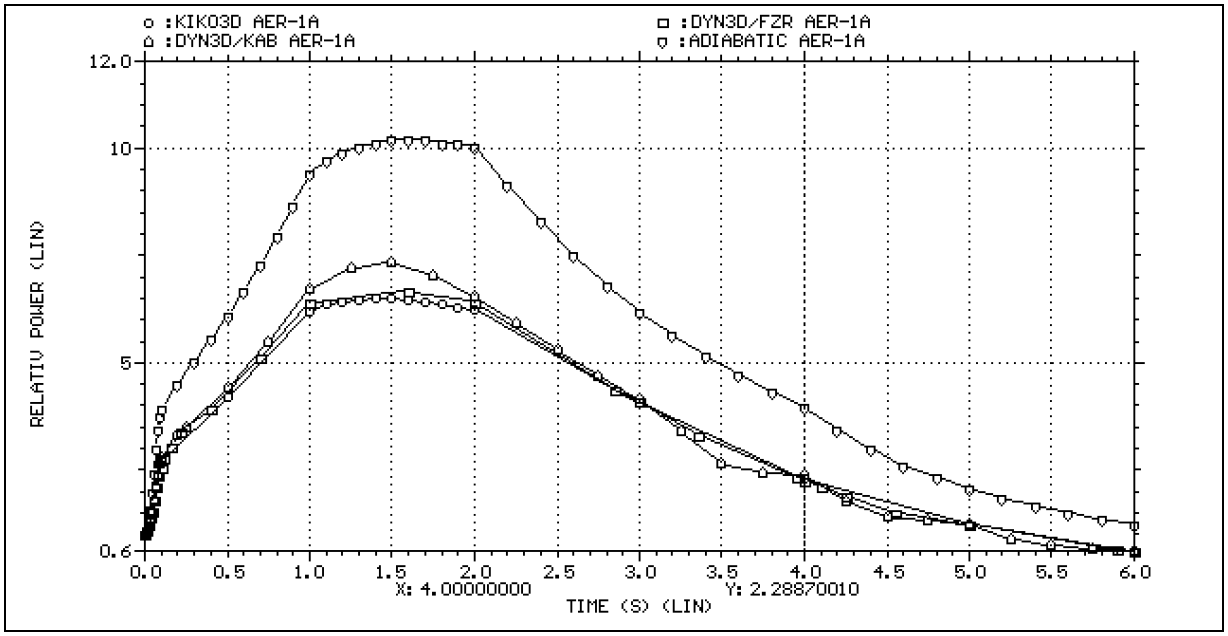

Fig. 6. Comparison of Relative Power in the AER-1A Benchmark

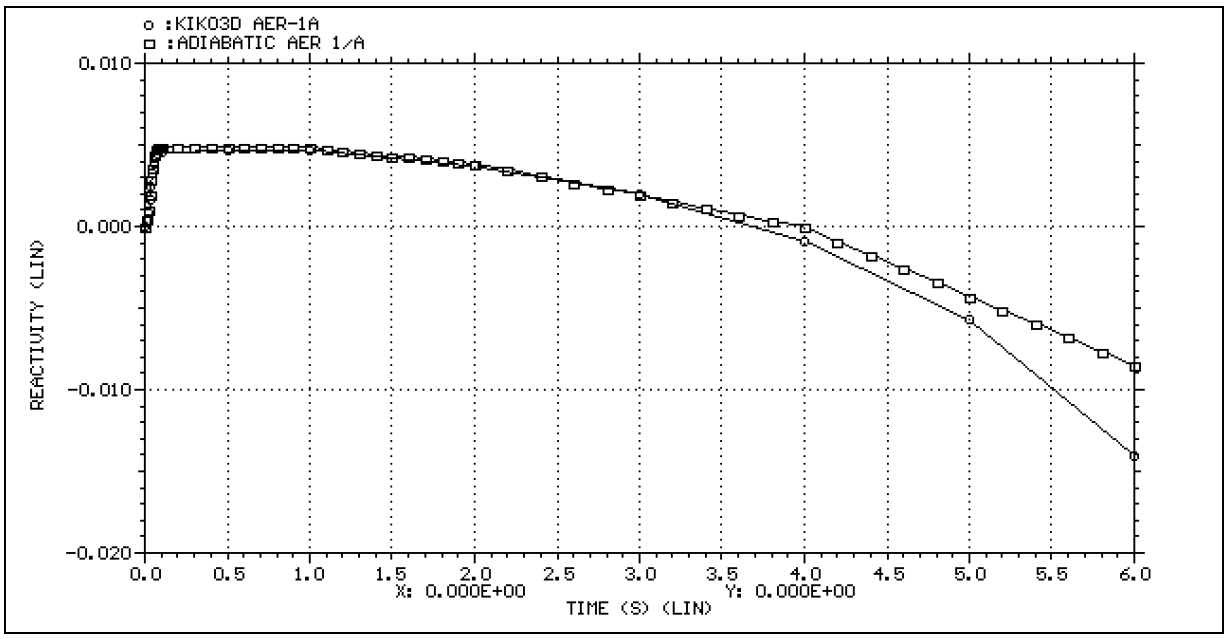

Fig. 7. Comparison of KIKO3D and Adiabatic Reactivity in the AER-1A Test Problem

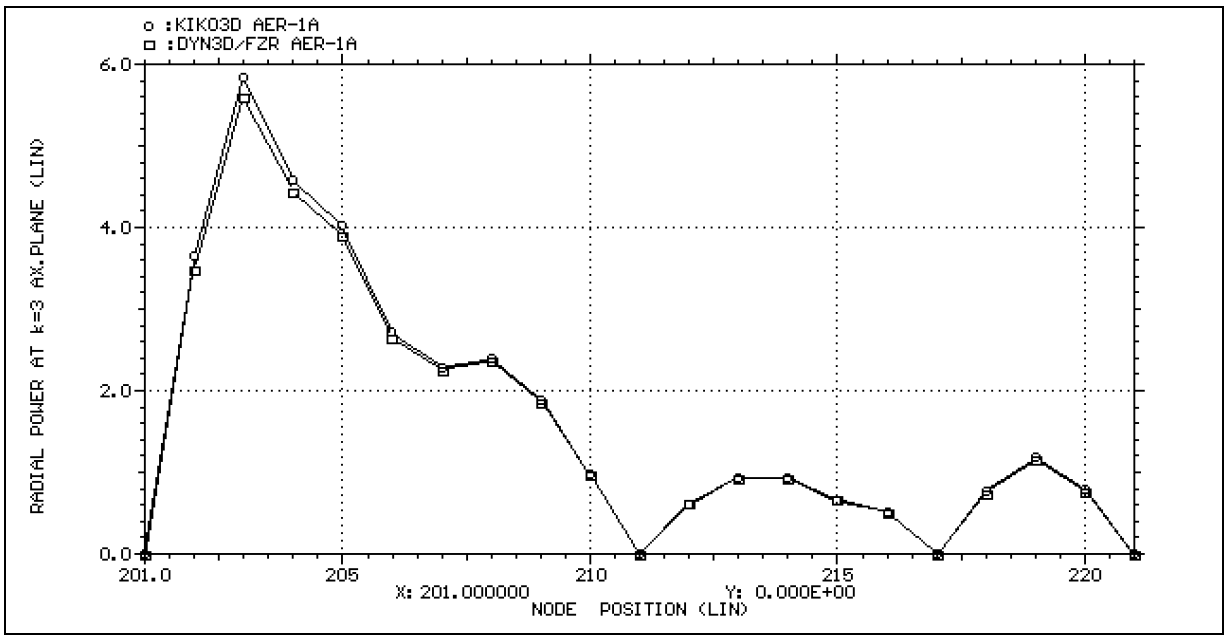

Fig. 8. Comparison of Asymmetric Radial Power Distributions at the End of AER-1B Transient Through the Horizontal Symmetry Line of the Core

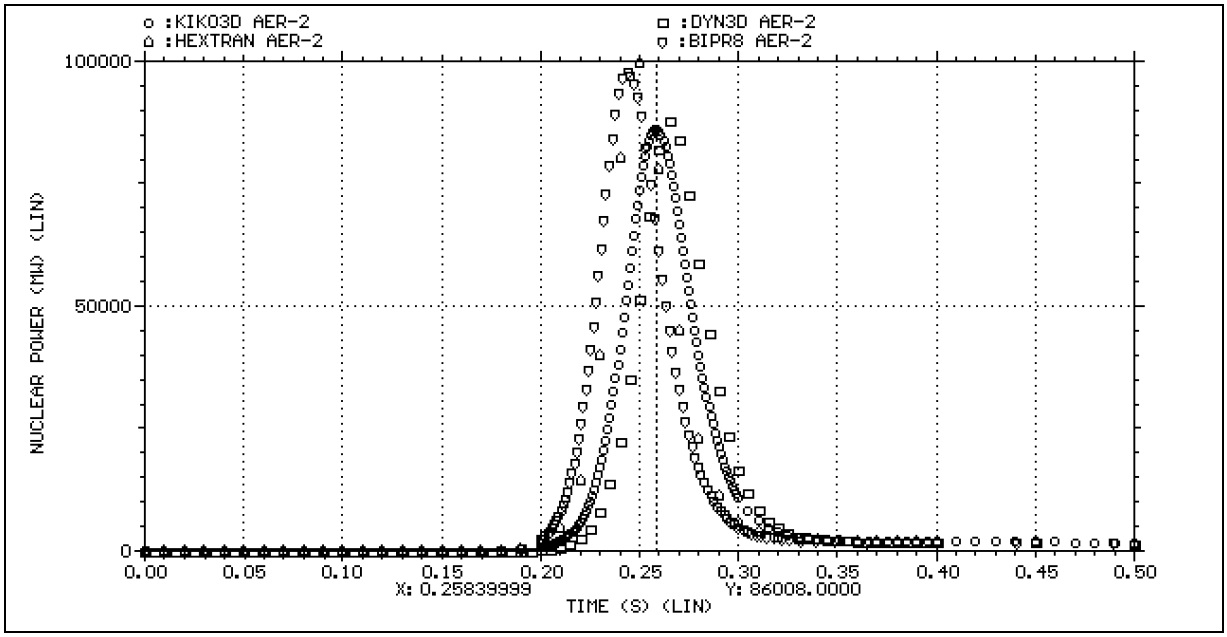

Fig. 9. Comparison of Nuclear Power in the AER-2 Benchmark

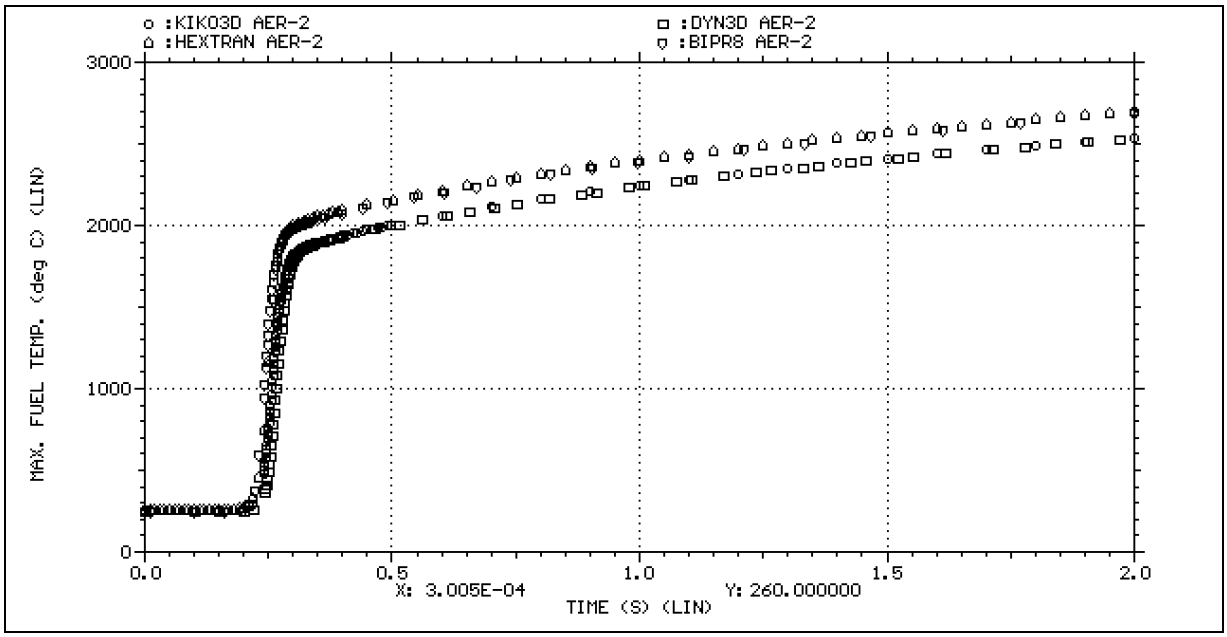

Fig. 10. Comparison of Maximum Fuel Temperatures in the AER-2 Benchmark

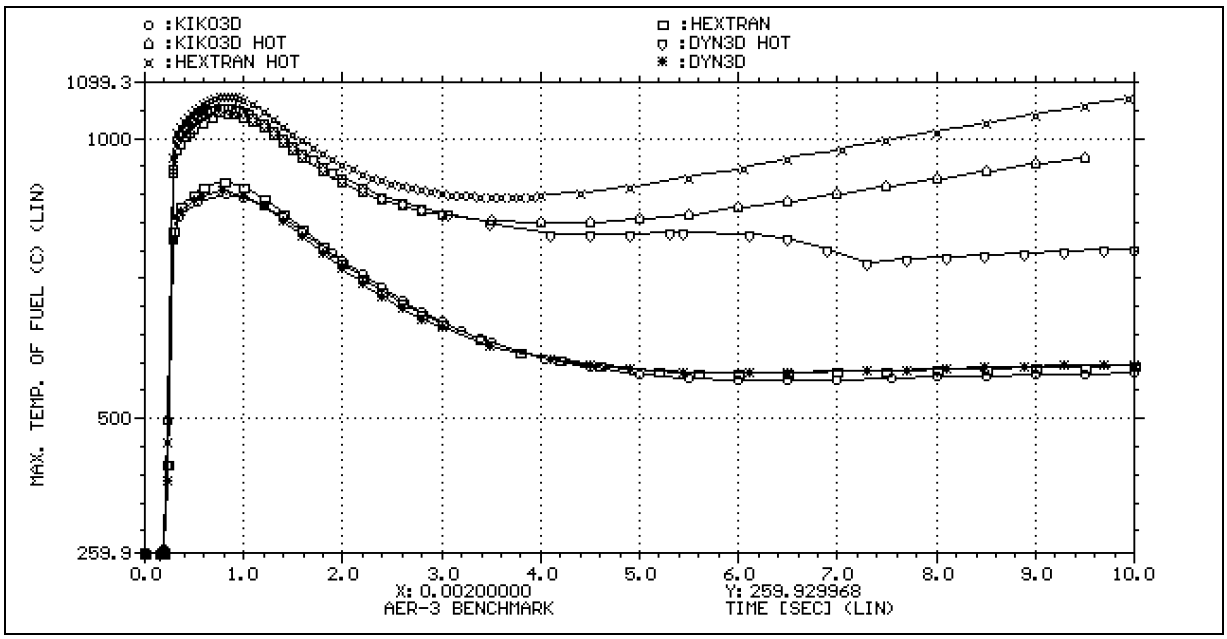

Fig. 11. Comparison of Maximum Node-Wise Fuel Center-Line Temperatures in Core Calculation and in the Hot Channel Calculation Belonging to K_x=1.25 Excess Power Peaking Factor. AER-3 Benchmark

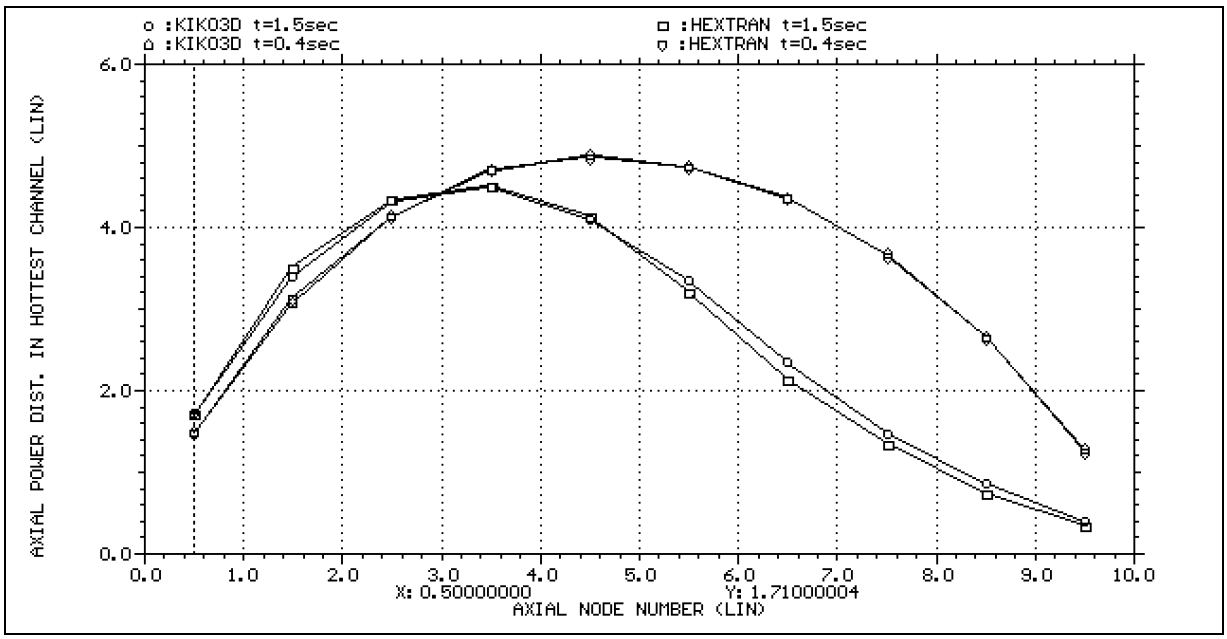

Fig. 12. Comparison of Axial Power Density Distributions in the Hottest Assembly at t=0.4 s and t=1.5 s in the AER-3 Benchmark

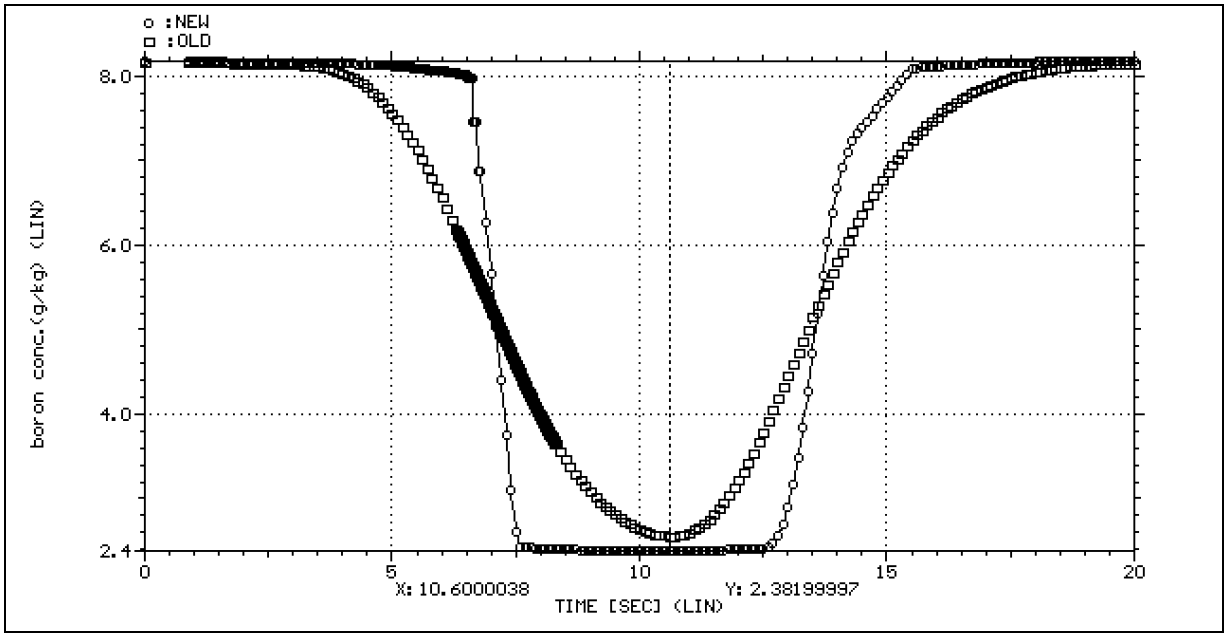

Fig. 13. Boron Concentration at the 9-th Axial Layer in the Core from KIKO3D with the Old Traditional and with the New Improved Boron Transport Model; AER-4 Benchmark

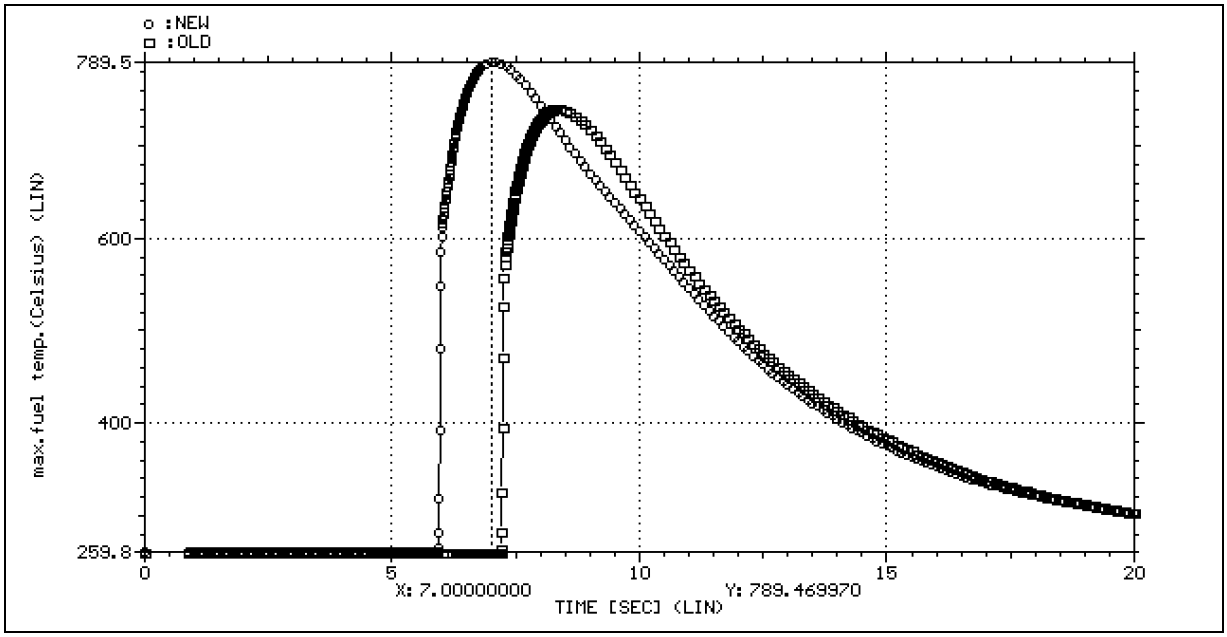

Fig. 14. Maximum Fuel Center-Line Temperature from KIKO3D with the Old Traditional and with the New Improved Boron Transport Model; AER-4 Benchmark

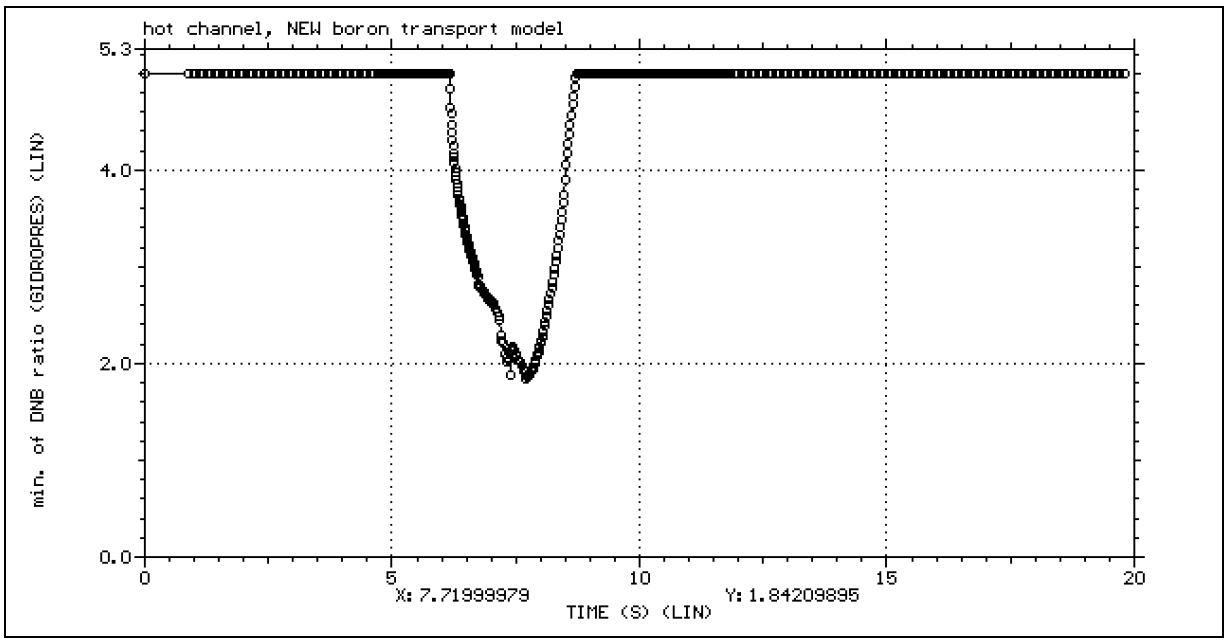

Fig. 15. Minimum of DNB Ratio in the Hot Channel Calculation According to KIKO3D Results with the New Improved Boron Transport Model; AER-4 Benchmark